



Published in final edited form as:

J Biol Chem. 2007 October 19; 282(42): 30974–30984. doi:10.1074/jbc.M704861200.

Leucine Carboxyl Methyltransferase-1 Is Necessary for Normal Progression through Mitosis in Mammalian Cells*

Jocelyn A. Lee and David C. Pallas¹

Department of Biochemistry, Winship Cancer Center, and Biochemistry, Cell, and Developmental Biology Program, Emory University School of Medicine, Atlanta, Georgia 30322

Abstract

Protein phosphatase 2A (PP2A) is a multifunctional phosphatase that plays important roles in many cellular processes including regulation of cell cycle and apoptosis. Because PP2A is involved in so many diverse processes, it is highly regulated by both non-covalent and covalent mechanisms that are still being defined. In this study we have investigated the importance of leucine carboxyl methyltransferase-1 (LCMT-1) for PP2A methylation and cell function. We show that reduction of LCMT-1 protein levels by small hairpin RNAs causes up to a 70% reduction in PP2A methylation in HeLa cells, indicating that LCMT-1 is the major mammalian PP2A methyltransferase. In addition, LCMT-1 knockdown reduced the formation of PP2A heterotrimers containing the B α regulatory subunit and, in a subset of the cells, induced apoptosis, characterized by caspase activation, nuclear condensation/fragmentation, and membrane blebbing. Knockdown of the PP2A B α regulatory subunit induced a similar amount of apoptosis, suggesting that LCMT-1 induces apoptosis in part by disrupting the formation of PP2A_{B α AC} heterotrimers. Treatment with a pancaspase inhibitor partially rescued cells from apoptosis induced by LCMT-1 or B α knockdown. LCMT-1 knockdown cells and B α knockdown cells were more sensitive to the spindle-targeting drug nocodazole, suggesting that LCMT-1 and B α are important for spindle checkpoint. Treatment of LCMT-1 and B α knockdown cells with thymidine dramatically reduced cell death, presumably by blocking progression through mitosis. Consistent with these results, homozygous gene trap knock-out of LCMT-1 in mice resulted in embryonic lethality. Collectively, our results indicate that LCMT-1 is important for normal progression through mitosis and cell survival and is essential for embryonic development in mice.

Protein phosphatase 2A (PP2A),² a multifunctional serine/threonine phosphatase, has been implicated in the regulation of cell growth and proliferation, primarily at the G₂/M transition, and in the development of human cancers (1). PP2A is composed of three functionally distinct subunits: A (structural), B-type (regulatory/targeting), and C (catalytic). Binding of different B-type subunits to the core PP2A heterodimer (A/C) alters its substrate

*This work was supported by NCI, National Institutes of Health Grant CA57327 (to D. C. P.) and Predoctoral Fellowship Award CA1236402 (to J. A. L.).

© 2007 by The American Society for Biochemistry and Molecular Biology, Inc.

To whom correspondence should be addressed: Dept. of Biochemistry, Emory University School of Medicine, 1510 Clifton Rd., Atlanta, GA 30322. Tel.: 404-727-5620; Fax: 404-727-2738; dpallas@emory.edu.

¹Under agreements between Upstate Biotechnology Inc. (Millipore), Santa Cruz Biotechnologies, Stratagene, Inc., and Emory University, David Pallas is entitled to a share of sales royalty received by the University from these companies. In addition, this same author serves as a consultant to Millipore. The terms of this arrangement have been reviewed and approved by Emory University in accordance with its conflict of interest policies.

²The abbreviations used are: PP2A, protein phosphatase 2A; LCMT-1, leucine carboxyl methyltransferase-1; shRNA, small hairpin RNA; B α , PP2A B55 α ; C subunit, PP2A catalytic subunit; A subunit, PP2A structural subunit; HA, hemagglutinin; AFC, aminofluoromethylcoumarin; DAPI, 4',6-diamidino-2-phenylindole; z-, benzyloxycarbonyl; fmk, fluoromethyl ketone; VC, vector control; ES, embryonic stem.

specificity and targets PP2A to different substrates and subcellular locations. Although there are two genes each for the C and A subunits in mammalian cells, there are multiple families of B-type subunits ((B (B55/PR55), B' (B56/PR61), B'' (PR72)) and a putative B''' (striatin) family, each of which has multiple members (1). Thus, a variety of heterotrimeric PP2A holoenzymes exist that differ primarily in their regulatory/targeting B-type subunits. In addition, Polyomavirus middle tumor antigen and Polyomavirus and SV40 small tumor antigens act as viral B-type subunits, displacing certain cellular B-type subunits and binding to the PP2A core heterodimer, altering its activity (Refs. 2–9 and references therein).

Reversible methylation is one of the most specific cellular mechanisms known for regulating PP2A and, thus, may have promise as a mechanism-based therapeutic target. In mammalian cells PP2A is methylated on its catalytic subunit carboxyl-terminal leucine (Leu-309) α -carboxyl group by leucine carboxyl methyltransferase-1 (LCMT-1) (10–16) and is demethylated by protein phosphatase methylesterase-1 (17–19). Methylation indirectly regulates PP2A function by altering the formation of PP2A holoenzymes, thus influencing the subcellular targeting and specificity of PP2A (8, 20–25). C subunit methylation has a differential effect on incorporation of different B-type subunits into PP2A holoenzymes. In *Saccharomyces cerevisiae*, where there is only one B subunit (Cdc55p) and one B' subunit (Rts1p), methylation increases the formation of heterotrimers containing B subunit 20-fold while increasing B' heterotrimer formation less than 2-fold (26). In mammalian cells, methylation is important for efficient assembly of B α AC heterotrimers (22, 24) but is not necessary for formation of PP2A complexes containing striatin family members or the viral B-type subunit, Polyomavirus middle tumor antigen (24). Based on experiments with a PP2A C subunit lacking leucine 309, methylation may differentially affect different B' family members in mammalian cells as well (27).

Based on these data, loss of PP2A methylation would be predicted to have the greatest effect on the function of PP2A heterotrimers containing the B/B55 family of regulatory subunits (PP2A_{BAC}). PP2A_{BAC} trimers have been implicated in mitosis promoting factor (MPF/Cdk1-cyclin B1) regulation in *Xenopus* (28) and in the regulation of mitotic exit in yeast (29–31). Therefore, PP2A methylation may regulate entry into mitosis as well as mitotic progression and exit. Consistent with this possibility, the level of PP2A methylation has been reported to change in a cell cycle-dependent manner in rat and human cells (32, 33). PP2A_{BAC} heterotrimers have also been shown to be essential in yeast for spindle checkpoint (34) and to regulate phosphorylation and degradation of human securin (35). In accord with this necessity for PP2A_{BAC} heterotrimers, we and others have shown that PP2A methylation is required for spindle checkpoint in yeast as indicated by increased sensitivity of PP2A methyltransferase-disrupted cells to spindle-targeting drugs like nocodazole (23, 25). However, it is not known if PP2A methylation is important for regulation of mitosis in mammalian cells. In fact, nothing is known about the role of LCMT-1 or protein phosphatase methylesterase-1 in mammalian cell growth and proliferation, including whether LCMT-1 is the major PP2A methyltransferase *in vivo*. In this study we used lentiviral small hairpin RNA (shRNA) vectors to knock down LCMT-1 expression and investigate the importance of LCMT-1 in mammalian cells. We also tested whether LCMT-1 was necessary for embryonic development in mice. Collectively, our results indicate that LCMT-1 is the major PP2A methyltransferase in mammalian cells, that LCMT-1 is important for normal progression through mitosis and for cell survival, and that it is required for mouse embryonic development.

EXPERIMENTAL PROCEDURES

Antibodies

LCMT-1 was detected using an affinity-purified rabbit anti-LCMT-1 polyclonal antibody, RK3110, generated against a 17-amino acid peptide corresponding to residues 173–189 of human LCMT-1. PP2A B α and C subunit were detected with mouse monoclonal antibodies from Upstate Bio-technology (clone 2G9) and BD Transduction Laboratories, respectively. Unmethylated PP2A C subunit was detected with a previously described (24) mouse monoclonal antibody (clone 4B7; available from Upstate Biotechnology, Stratagene and Santa Cruz Biotechnology). Methylated PP2A C subunit was detected with 2A10 mouse monoclonal antibody (Upstate Biotechnology, Inc.). HA-tagged proteins were immunoprecipitated and immunoblotted with the mouse monoclonal antibodies 12CA5 (available from Santa Cruz Biotechnology, Inc.) and 16B12 (Covance Research Products), respectively.

Cell Culture and the Creation of Stable Lines That Express LCMT-1- and B α -directed shRNAs

HeLa cervical carcinoma cells were obtained from American Type Culture Collection. HCT116 colon cancer cells were obtained from Dr. Eva Schmeltz. Both lines were maintained in Dulbecco's modified Eagle's medium supplemented with 10% fetal bovine serum. To create HeLa and HCT116 lines that stably express LCMT-1- or PP2A B α -directed shRNAs, cells were infected with lentiviruses expressing shRNAs. These lentiviruses were generated using a three-plasmid-based lentivirus system (36) (available from The RNAi Consortium (TRC) at the Broad Institute). The targeted sequences in the shRNA lentiviruses we used were: L2, 5'-GCCATGTTTCATAAACTACGAA-3' (TRC ID TRCN0000035060); L3, 5'-CGTCGACATGATGGAGTT-GTA-3' (TRC ID TRCN0000035061); B α , 5'-GCAAGTGGC-AAGCGAAAGAAA-3' (TRC ID TRCN000002493). After infection with the appropriate lentivirus, cells were selected with puromycin (2 μ g/ml) until a canary dish of uninfected parental cells was completely dead (usually 3 days). After incubating one additional day to allow the cells to recover from puromycin treatment, cells were then used for experiments, and aliquots of cells were frozen for later use. Cells were used within 10 days after selection/thawing.

Determination of the Level of PP2Ac Methylation

The steady-state level of PP2A catalytic subunit methylation was measured in lysates with a monoclonal antibody specific for unmethylated PP2A C subunit (4b7) using our published method (24), which is described in the legend to Fig. 1, B and C, in the current study. Quantitation of the 4b7 signal was performed with a Bio-Rad Fluor S-Max Chemilumimager and Bio-Rad Quantity One Software.

Cell Transfections and Immunoprecipitations

The pCEP4 HA-tagged B α construct was obtained from the laboratory of Dr. David M. Virshup (Department of Pediatrics and of Oncological Sciences, University of Utah). Vector control HeLa cells and HeLa cells that stably express shRNAs directed to LCMT-1 (L3) were plated at a density of 3.5×10^5 cells/60-mm dish and then transfected with pCEP4 HA-tagged B α using FuGENE6 transfection reagent (Roche Diagnostics). At 72 h post-transfection, cells were lysed in an Nonidet P-40-containing lysis buffer (10% glycerol, 20 mM Tris, pH 8.0, 137 mM NaCl, 1% Nonidet P-40), and immunoprecipitation of N-terminally HA-tagged B α was carried out with anti-HA tag monoclonal antibody, 12CA5, covalently cross-linked to protein A-Sepharose beads. To determine the amount of PP2A C subunit associated with each of the immunoprecipitated samples, the immunoprecipitates

were analyzed by SDS-PAGE and immunoblotted with 16B12 anti-HA tag antibody and with anti-PP2A C subunit antibody, and then the relative amount of HA-tagged B α and PP2A C subunit were determined by quantitation using a Bio-Rad Fluor S-Max Chemilumimager and Bio-Rad Quantity One Software.

Analysis of Cell Viability by Trypan Blue Exclusion

Vector control cells and cells that stably express shRNAs directed toward LCMT-1 (L2 or L3) or B α were plated at a density of 2×10^4 cells/well in a 12-well dish, allowed to adhere overnight, washed to remove dead cells, and then incubated for 24 h at 37 °C. Cells were then harvested and checked for viability by trypan blue exclusion (0.4% trypan blue).

Analysis of DNA Condensation and Fragmentation Using DAPI Stain

Vector control HeLa cells and HeLa cells that stably express shRNAs directed toward LCMT-1 (L2 or L3) or B α were plated at a density of 2×10^4 cells/well in a 12-well dish, allowed to adhere overnight, washed to remove dead cells, and then incubated for 24 h at 37 °C. Cells were then incubated with DAPI stain for 5 min at 37 °C. Cells were subsequently observed by fluorescence microscopy using an Olympus IX81 phase/fluorescence microscope and analyzed using Slidebook Microscope Analysis software (Intelligent Imaging, Inc.).

Caspase 3 in Cell Detection Assay

Vector control HeLa cells and HeLa cells that stably express shRNAs directed toward LCMT-1 (L2 or L3) or B α were plated at a density of 1.5×10^5 cells/well in a 6-well dish, allowed to adhere overnight, washed to remove dead cells, and then incubated for 24 h at 37 °C. Cells were then harvested and gently pelleted, washed in media, and then incubated in media containing Red-DEVD-fmk caspase-3 activity indicator (DEVD-fmk conjugated to sulforhodamine; Calbiochem) and 10% fetal calf serum for 1 h in a 37 °C incubator per the manufacturer's instructions. Cells were subsequently placed on a coverslip and observed by fluorescence microscopy using an Olympus IX81 phase/fluorescence microscope and analyzed using Slidebook Microscope Analysis software (Intelligent Imaging, Inc.).

z-DEVD-AFC Caspase 3 in Vitro Activity Assay

Vector control HeLa cells and HeLa cells that stably express shRNAs directed toward LCMT-1 (L2 or L3) or B α were plated at a density of 1.5×10^5 cells/well in a 6-well dish, allowed to adhere overnight, washed to remove dead cells, and then incubated for 24 h at 37 °C. Cells were then washed 3 times with $1 \times$ phosphate-buffered saline and incubated in a Nonidet P-40-containing lysis buffer (10% glycerol, 20 mM Tris, pH 8.0, 137 mM NaCl, 1% Nonidet P-40) for 20 min on ice. The cells were then sonicated on ice for 5×2 -s bursts. The supernatant was then centrifuged for 10 min at 13,000 μ g. The protein concentration of the supernatant was assayed by the Lowry method (Bio-Rad). 25 μ g of protein was incubated with z-DEVD-AFC (25 μ M) (Calbiochem substrate IV) at 37 °C for 1 h. Caspase activity was measured using a Wallac Victor² 1420 Multilabel Counter fluorimeter (PerkinElmer Life Sciences) at 405-nm excitation and 535-nm emission wavelengths.

Effect of Caspase Inhibition on Cell Viability

Vector control HeLa cells and HeLa cells that stably express shRNAs directed toward LCMT-1 (L2 or L3) or B α were plated at a density of 2×10^4 cells/well in duplicate 12-well dishes, allowed to adhere overnight, washed to remove dead cells, and then incubated with z-VAD-fmk pancaspase inhibitor (50 μ M; BioMol) or with vehicle only for 24 h at 37 °C. Cells were then harvested and checked for viability by trypan blue exclusion (0.4% trypan blue), and the viability of each line \pm caspase inhibitor was compared.

Phase Time-lapse Microscopy

Vector control HeLa cells and HeLa cells that stably express shRNAs directed toward LCMT-1 (L2 or L3) or B α were plated at a density of 4×10^4 cells/well in a 6-well dish, allowed to adhere overnight, washed to remove dead cells, and then incubated at 37 °C in a temperature and atmosphere-controlled microscope stage incubator (M6; Zeiss Instruments) on an Olympus IX81 phase/fluorescence microscope equipped with a computer-driven motorized stage (ASI). Phase images were captured every 6 min for 24–36 h. Images were analyzed using Slidebook Microscope Analysis software (Intelligent Imaging, Inc.).

Nocodazole Treatment and Analysis of Cell Viability

Cells were plated at a density of 2×10^4 cells/well into duplicate 12-well dishes, allowed to adhere overnight, and washed to remove dead cells, and then one dish was incubated with nocodazole (200 ng/ml) and the other with vehicle control for 24 h at 37 °C. Cells were then harvested and assayed for viability by trypan blue exclusion (0.4% trypan blue) to determine any change in cell death for each line due to the presence of nocodazole.

Thymidine Block and Analysis of Cell Viability

Cells were plated at a density of 2×10^4 cells/well into triplicate wells in duplicate 12-well dishes, allowed to adhere overnight, washed to remove dead cells, and then incubated with thymidine (2 mM) or vehicle only for 24 h at 37 °C. Cells were then harvested and checked for viability by trypan blue exclusion (0.4% trypan blue) to determine any change in cell death for each line due to G₁/S arrest induced by thymidine treatment.

Generation of LCMT-1 Knock-out Mice and Genotyping

LCMT 1+/- embryonic stem cells containing a gene trap insertion in the first intron of the LCMT1 locus were obtained from German Gene Trap Consortium, Neuherberg, Germany. These cells were expanded in culture and were injected into blastocysts from C57BL/6 donors using standard techniques by the Emory University School of Medicine Transgenic Mouse and Gene Targeting Core Facility. Resultant chimeric mice were bred to generate heterozygous F1 animals that were then intercrossed to determine whether homozygous knock-out of LCMT-1 was embryonic lethal.

RESULTS

Down-regulation of LCMT-1 Causes a Substantial Decrease in PP2Ac Methylation

To determine whether LCMT-1 was necessary for cell viability and normal cell cycle progression in mammalian cells, we decreased LCMT-1 expression in HeLa cells by stably expressing shRNAs to LCMT-1 via lentiviral vectors. Fig. 1A shows that two different LCMT-1 shRNAs, designated L2 and L3, were able to dramatically reduce LCMT-1 protein levels.

In yeast, loss of the LCMT-1 homolog, Ppm1p, results in loss of PP2A (Pph21p/Pph22p) methylation, indicating that Ppm1p is probably solely responsible for methylating PP2A under normal growth conditions (23, 25, 37). Although LCMT-1 has been shown to methylate PP2A *in vitro* (10–16), its contribution to PP2A methylation *in vivo* has not been quantitatively examined in mammalian cells. To determine the contribution of LCMT-1 to PP2A methylation in mammalian cells, we quantitated the steady-state levels of PP2Ac methylation in L2 and L3 LCMT-1 knockdown cells using our monoclonal antibody, 4b7, which is specific for unmethylated PP2A catalytic subunit (see “Experimental Procedures” and the legend for Fig. 1) (24). Fig. 1, B and C, show that the knockdown of LCMT-1 by L2 and L3 shRNAs caused a substantial (32 or 71%, respectively) reduction in PP2A catalytic

subunit methylation in HeLa cells as compared with vector control (VC) cells. Interestingly, although LCMT-1 could not be detected easily in either the L2 or L3 cells (Fig. 1A), L3 was more efficient than L2 at reducing PP2A methylation (Fig. 1C). To further corroborate our results with the 4b7 anti-unmethylated PP2A catalytic subunit antibody, we performed a separate experiment in which we analyzed vector control and L3 LCMT-1 knockdown cells with another monoclonal antibody (2A10) that is specific for methylated PP2A catalytic subunit. The results in Fig. 1D show that 2A10 also detected a large reduction in methylated PP2A catalytic subunit in L3 LCMT-1 knockdown cells. Quantitation of results from two separate experiments showed that PP2A C subunit methylation was reduced >3-fold. Collectively, these results show that mammalian LCMT-1 is responsible for the majority of PP2A methylation, similar to the case for the *S. cerevisiae* LCMT-1 homolog, Ppm1p. They also demonstrate that the small amount of residual LCMT-1 protein in the L2 and L3 knockdown cells may be sufficient for methylating 25–60% of the PP2A in these cells.

Knockdown of LCMT-1 Greatly Reduces PP2A Ba Binding to C Subunit

In yeast, deletion of the gene encoding Ppm1p dramatically reduces the binding of PP2A B subunit to C subunit. We wanted to determine whether knockdown of LCMT-1 had similar effects on Ba binding to C subunit in mammalian cells. Because no antibody capable of immunoprecipitating endogenous Ba/C subunit complexes was available, we assayed the ability of transfected HA-tagged Ba (HA-Ba) to associate with endogenous C subunit in our vector control and L3 LCMT-1 shRNA HeLa cells. Fig. 2, A and B, show that methylation was greatly reduced in the L3 cells used for this experiment. Fig. 2, C and D, show that down-regulation of LCMT-1 by L3 shRNA greatly reduced C subunit association with HA-Ba. Thus, LCMT-1 is important for PP2A_{BaAC} trimer formation in mammalian cells.

Knockdown of LCMT-1 Induces Cell Death

In mammalian cells PP2A plays important roles in both cell cycle control and in apoptosis. We, therefore, analyzed the LCMT-1 knockdown cells and control cells to determine whether there was an effect of LCMT-1 knockdown on cell viability. After infection with L2 and L3 shRNA-expressing lentiviruses, we noticed that a portion of the HeLa cells knocked down for LCMT-1 was dying, whereas little to no death was seen in the cells infected with the control lentivirus. To determine the extent of death induced by LCMT-1 knockdown, we measured the percent of cells in each of these lines that died during a 24-h period in culture. Fig. 3A shows that both L2 and L3 shRNA knockdown HeLa cells had significantly more death (7–8%) during this period than the vector control cells (1%).

Because the stable formation of PP2A trimers containing the Ba regulatory subunit has been shown to be highly dependent on methylation of the PP2A C subunit (22, 24) and we showed above that Ba/C subunit complexes were reduced in LCMT-1 knockdown cells, it was possible that the cell death seen in L2 and L3 knockdown cells was due in part to impairment of PP2A_{BaAC} trimer formation and function. We, therefore, tested whether knockdown of Ba would also induce death. Indeed, knockdown of Ba by a lentiviral shRNA vector, demonstrated in Fig. 3B, also caused an increase in cell death comparable with that induced by knocking down LCMT-1 (Fig. 3A). Although the increase in cell death in Ba knockdown cells was more variable than for L2 and L3, it was statistically significant ($p < 0.05$).

Knockdown of LCMT-1 Induces Caspase-dependent and Caspase-independent Cell Death

To begin to characterize the mechanism of death induced by knockdown of LCMT-1 or Ba, we analyzed our vector control, L2, L3, and Ba shRNA cells by phase time-lapse microscopy. In comparison to vector control cells, L2, L3, and Ba knockdown cells

exhibited increased membrane blebbing (Fig. 4A and data not shown), a characteristic of caspase-mediated cell death (38). To further analyze this cell death, we next incubated each cell line with DAPI stain to detect condensed and fragmented DNA, which is also characteristic of apoptosis (39). Fig. 4B shows that LCMT-1 or B α knockdown induced DNA condensation and fragmentation, supporting the idea that reduction of LCMT-1 induces apoptosis, perhaps in part by inhibition of B α function.

Because the membrane blebbing observed in our knockdown cells is a characteristic of caspase activation (38), we wanted to determine whether LCMT-1 and B α knockdown induce caspase activation. We first assayed caspase activation in live vector control, LCMT-1 knockdown, and B α knockdown cells. Vector control cells treated with the pankinase inhibitor staurosporine were used as a positive control (40). The cell-permeable substrate we used for this assay, Red-DEVD-fmk, is a preferred substrate of caspases 3 and 7 but also can serve as a substrate for a number of other caspases (41). Fig. 4C shows that knockdown of LCMT-1 by either L2 or L3 shRNA caused an increase in caspase activity *in vivo*. Although knockdown of B α consistently induced a small increase in caspase activation as detected by this assay, the increase was not statistically significant (Fig. 4C and data not shown). In a complementary approach, we assayed for caspase activity in lysates of our vector control and LCMT-1 and B α knockdown cells using the caspase substrate z-DEVD-AFC. Again, staurosporine-treated vector control cells were used as a positive control. The results we obtained (Fig. 4D) are consistent with our results from the *in vivo* caspase assay. Knockdown of LCMT-1 by either L2 or L3 shRNA caused significant activation of caspases in three independent experiments. Knockdown of B α on the other hand caused some caspase activation in all experiments, but only in one experiment was this increase significant (Fig. 4D and data not shown).

Although this result indicates that caspases are activated at least in the case of LCMT-1 knockdown cells, it does not show whether caspase activation is necessary for the observed apoptosis. To test whether the observed death requires caspase activation, we treated our LCMT-1 (L2 and L3) and B α knockdown cells with the pancaspase inhibitor z-VAD-fmk (50 μ M) to see if it would reduce cell death. Interestingly, we observed a reduction in cell death in all three knockdown cell lines (L2, L3, and B α shRNA cells) as compared with vector control, but consistent with our caspase activation results, the reduction in cell death was always the least for the B α knockdown cells (Fig. 4E and data not shown). These results suggest that down-regulation of LCMT-1 or B α causes death by both caspase-dependent and caspase-independent pathways but that LCMT-1 knockdown causes more caspase-dependent cell death than B α knockdown.

LCMT-1 or B α Knockdown Causes Nocodazole Sensitivity

In our initial experiments using phase time-lapse microscopy, we found that a subset of LCMT-1 knockdown cells round up as if to enter mitosis, sometimes with a visible metaphase plate, and remain rounded for longer than expected for a normal mitosis, eventually undergoing apoptosis. Fig. 5 shows an example of such a cell that enters mitosis (metaphase plate is clearly visible in the cell at the 1.6h time point) and remains rounded until membrane blebbing begins ~14 h later. In yeast, we and others have shown that deletion of the gene *PPM1*, which encodes the yeast homolog of LCMT-1, or deletion of the gene *CDC55*, which encodes the yeast homolog of B α , has no effect on cell viability under normal growth conditions unless the cells are sensitized by the microtubule-depolymerizing drug nocodazole, a phenotype characteristic of a spindle checkpoint defect (23, 25, 29, 34). To determine whether LCMT-1 and/or B α knockdown results in a similar mitotic defect in mammalian cells as in yeast, we treated our LCMT-1 (L2 and L3) and B α knockdown cells for 24 h with nocodazole (200 nM) and then assayed these cells to determine whether there were any changes in the amount of death as compared with untreated cells. The results in

Fig. 6A show that although nocodazole treatment only caused a 1% increase in cell death in vector control cells, it induced a much greater increase in death in cells with reduced LCMT-1 levels (10–13%). Moreover, reduction of $B\alpha$ levels also resulted in increased death in the presence of nocodazole (Fig. 6A).

Thymidine Treatment Rescues Cell Death Caused by LCMT-1 or $B\alpha$ Knockdown

To determine whether the increased death caused by nocodazole was specifically caused by arresting cells in mitosis (and, thus, perhaps a spindle checkpoint defect) or was just due to cell cycle arrest, we also treated our vector control, LCMT-1, and $B\alpha$ knockdown cells with thymidine, which has been used as a cell synchronization agent to arrest cells in G_1/S . Strikingly, thymidine treatment caused a dramatic reduction in cell death in both LCMT-1 (L2 and L3) and $B\alpha$ knockdown cells (Fig. 6), indicating that the increased cell death observed when cells are treated with nocodazole is specific to mitosis.

LCMT-1 Knockdown Also Causes Increased Death of HCT116 Colon Cancer Cells in Nocodazole

Increased sensitivity of HeLa LCMT-1 knockdown cells to nocodazole (Fig. 6A) suggested that LCMT-1 plays a role in spindle checkpoint and that drugs targeting LCMT-1 might have potential in combination chemotherapy with microtubule-targeting drugs. We wanted to determine next whether LCMT-1 knockdown would cause increased killing of another cancer cell type in nocodazole. The results presented in Fig. 7, A–C, show that L2 and L3 shRNAs also reduce LCMT-1 protein levels and PP2A methylation in HCT116 cells. Decreased methylation in the L2 and L3 cells was detected both by immunoblotting with 2A10 antibody specific for methylated PP2A catalytic subunit (Fig. 7A) and by using our methylation assay employing our monoclonal antibody specific for unmethylated PP2A catalytic subunit (Fig. 7, B and C). Importantly, Fig. 7D shows that HCT116 L2 and L3 LCMT-1 knockdown cells were more sensitive to nocodazole than were vector control cells. Similar to the results obtained for HeLa cells (Fig. 6A), an average increase in percent killing of 9% in nocodazole was seen with L2 and L3 shRNAs in three separate experiments, whereas vector control cells only showed an average increase in killing of 1.5% in the same experiments (Fig. 7D and data not shown).

Homozygous Knock-out of LCMT-1 in Mice Causes Embryonic Lethality

Because our data indicated that LCMT-1 was necessary for normal progression through mitosis, we predicted that LCMT-1 knock-out would be embryonic lethal. To test this hypothesis, we generated an LCMT-1 knock-out mouse using LCMT-1^{+/-} embryonic stem (ES) cells created by The German Gene Trap Consortium and tested whether live LCMT-1^{-/-} pups could be obtained from crossing LCMT-1^{+/-} mice with each other. Our results are shown in Fig. 8. Fig. 8A shows that our genotyping primer sets for wild-type LCMT-1 and for gene trap knock-out LCMT-1 both produce robust products using DNA from the original LCMT-1^{+/-} ES cells or from progeny LCMT-1^{+/-} or LCMT-1^{+/+} mice obtained from breeding. Fig. 8, B and C, show that LCMT-1 protein was reduced about 2-fold in the LCMT-1^{+/-} ES cell line relative to control parental ES cells. Finally, Fig. 8D shows the average number of pups with each possible genotype obtained from eight LCMT-1^{+/-} × LCMT-1^{+/-} matings. If homozygous LCMT-1 loss had no effect on development, one would expect equal numbers of LCMT-1^{+/+} and LCMT-1^{-/-} mice. However, although 19 LCMT-1^{+/+} mice and 26 LCMT-1^{+/-} pups were born from these +/- × +/- crosses, no LCMT-1^{-/-} pups were obtained from any of the crosses, indicating that loss of LCMT-1 is indeed embryonic lethal.

DISCUSSION

Carboxyl methylation of PP2A was discovered well over a decade ago, but its function remained obscure until the discovery that the addition and removal of the single methyl group on the PP2A carboxyl-terminal leucine could differentially regulate the assembly of certain PP2A heterotrimers (22–25). The cloning of LCMT-1 as a mammalian PP2A methyltransferase by De Baere *et al.* (16) has facilitated the investigation the contribution of this enzyme toward PP2A methylation and function. However, until the recent advent of small interfering RNA approaches for mammalian cells, much advancement in our understanding has come from experiments performed in yeast because of the ease of performing genetic analyses. In fact, before this study, nothing was known about the importance of LCMT-1 for normal cell cycle progression and cell survival. In this report we have utilized lentiviral shRNA and Genetrap knock-out approaches to investigate LCMT-1 function in mammalian cells. We show that a strong reduction in LCMT-1 not only results in a substantial reduction in PP2A methylation in mammalian cells but also causes a decrease in B α subunit association with C subunit, induces apoptosis as evidenced by caspase activation, membrane blebbing, nuclear condensation and fragmentation, and cell death, and sensitizes HeLa and HCT116 cancer cells to the microtubule targeting drug nocodazole.

Although LCMT-1 was originally purified as a PP2A methyltransferase, only a small percentage of PP2A methyltransferase activity in the original cell extract was recovered (16), leaving open the question as to whether LCMT-1 is the major PP2A methyltransferase in mammalian cells. Our result showing that reduction of the steady-state level of PP2A C subunit methylation an average of 70% in HeLa cells and 63% in HCT116 cells by the LCMT-1 L3 shRNA clearly indicates that it is. Our observation that cells with ~10% of their normal amount of LCMT-1 protein have 30–70% of their normal amount of PP2A methylation suggests that either there is a second PP2A methyltransferase that is a minor contributor to PP2A methylation under normal growth conditions or cells have an excess of LCMT-1 for maintaining steady-state methylation levels of PP2A under cell culture conditions. The most obvious candidate for an additional PP2A methyltransferase would be the only known homolog of LCMT-1, LCMT-2. LCMT-2 was originally cloned by De Baere *et al.* (16), who showed that it could not methylate PP2A *in vitro*. Consistent with this *in vitro* mammalian result, a LCMT-2 homolog exists in yeast that does not seem to contribute detectably to PP2A methylation *in vivo* (23, 25, 37). These results suggest that LCMT-2 is not a PP2A methyltransferase. However, it still needs to be tested *in vivo* whether LCMT-2 contributes to PP2A methylation in mammalian cells. One possible explanation for the apparent excess of LCMT-1 is that it may be necessary for dynamic responses to cellular needs or for methylation of a currently unknown additional LCMT-1 substrate. Other possible LCMT-1 substrates include the PP2A-related phosphatases PP4 and PP6. Both of these phosphatases share ~60% amino acid identity with PP2A and have identical carboxyl-terminal amino acids, including a carboxyl-terminal leucine, the known site of carboxyl methylation for both PP2A and PP4 (42). Whether PP6 is methylated is not known. Further experiments will be necessary to determine whether LCMT-1 (or LCMT-2) methylates PP4 and/or PP6.

We have previously shown that B α is the PP2A B-type regulatory subunit whose assembly into heterotrimers is most dependent on PP2A C subunit methylation (24). Our current coimmunoprecipitation results provide further support for this conclusion. LCMT-1 has been shown previously to associate with PP2A *in vitro* (22) and to methylate PP2A on its carboxyl-terminal leucine α carboxyl group (10–16). In this study we have demonstrated further that LCMT-1 down-regulation in mammalian cells reduces both PP2A C subunit methylation and the formation of PP2A_{B α AC} heterotrimers and that down-regulation of

these same heterotrimers by $B\alpha$ knockdown can cause part of the phenotypes seen with LCMT-1 knockdown. Moreover, we have previously shown that loss of PP2A_{BAC} heterotrimer formation results in selective loss of PP2A activity toward a PP2A_{BAC}-specific substrate (8). Thus, it is possible that the cell death induced by LCMT-1 down-regulation may be due in part to dysregulation of $B\alpha$ heterotrimer function. A similar amount of apoptosis resulted when protein levels of either $B\alpha$ or LCMT-1 were greatly reduced. Moreover, the pancaspase inhibitor z-VAD-fmk could prevent a portion of the cell death induced by down-regulation of either LCMT-1 or $B\alpha$, indicating that in both cases caspase-dependent and caspase-independent death pathways contribute to cell death. This similarity in the cell death observed with either LCMT-1 or $B\alpha$ reduction is again consistent with the possibility that LCMT-1 down-regulation induces death to some degree through $B\alpha$ dysregulation. However, cell death induced by down-regulation of these two proteins does not appear to be identical. It was more difficult to detect caspase activation *in vivo* and *in vitro* with $B\alpha$ knockdown cells, and the rescue by z-VAD-fmk was consistently lower for the $B\alpha$ knockdown cells than for LCMT-1 knockdown cells. These differences suggest that LCMT-1 knockdown has other effects independent of $B\alpha$ that contribute to cell death. In yeast, deletion of the gene that encodes the LCMT-1 homolog, Ppm1p, not only reduces the level of PP2A_{BAC} heterotrimers 20-fold but also causes a smaller reduction (~2-fold) in PP2A_{B'AC} heterotrimers (23, 25, 26). Therefore, one possible effect unique to LCMT-1 knockdown may be reduction of PP2A_{B'AC} heterotrimers. Other possible targets of LCMT-1 that have yet to be tested also exist, such as PP2A heterotrimers, formed by other members (β , γ , δ , ϵ) of the B/B55 regulatory subunit family or by PP2A B'' regulatory subunits and PP4 and/or PP6 complexes. Although apoptosis-relevant targets of LCMT-1 other than $B\alpha$ remain to be determined, our results clearly indicate that they exist.

The increased sensitivity of both LCMT-1 and $B\alpha$ knockdown cells to the spindle-targeting drug, nocodazole, suggests that both of these proteins are important in mammalian cells for the spindle checkpoint, which ensures proper spindle formation and chromosomal attachment before progression from metaphase to anaphase. The fact that cell death was largely rescued by thymidine block-induced arrest in G₁/S indicates that cell cycle arrest, which is induced in HeLa cells by either nocodazole or thymidine, is not the sensitizing factor. Instead, the effect is specific to mitosis. This death in nocodazole- and not in thymidine-treated cells is consistent with previous results from yeast showing that loss of the $B\alpha$ homolog, Cdc55p, or of the LCMT-1 homolog, Ppm1p, causes increased sensitivity to nocodazole. However, it was not known with the increased complexity of mammalian cells whether this phenotype would be found in this system, where there are multiple members of each B-type regulatory subunit family. In mammalian cells the mechanistic details of the roles of B-type subunits in spindle checkpoint and mitotic exit are just beginning to emerge. Both the B family isoform, B δ , and the B' family isoform, B' γ , have recently been identified as negative regulators of sister chromatid separation (35, 43). B δ was found to protect cohesins from degradation by stabilizing securin, a negative regulator of the cohesin protease, separase. B' γ was reported to protect cohesin degradation by binding to Shugoshin (hSgo1) and maintaining cohesins in a more stable, hypophosphorylated state. Our data suggest that $B\alpha$ is also a negative regulator of the spindle checkpoint in mammalian cells. Whether it plays yet another distinct role or shares responsibility for dephosphorylation of cohesins or securin is not known. Overexpression data such as those presented in the B δ /securin study do not rule out a similar role for $B\alpha$. Likewise, B' γ identification as an hSgo1 partner leaves open the possibility that other B-type subunits might also associate with Shugoshin proteins. Finally, a role for LCMT-1 in spindle checkpoint is consistent with a role for PP2A methylation in mitotic progression. Experiments are under way to explore this possibility further.

PP2A regulates apoptotic pathways both positively and negatively by targeting different substrates via its diverse regulatory subunits. Consequently, PP2A inhibitors and small interfering RNA down-regulation of PP2A C and A subunits have been reported to induce apoptosis or block apoptosis, depending on the system (44–50). In both *Drosophila* and mammalian cells, B56/B' subunits have been reported to have an anti-apoptotic role (45, 46, 48). Some evidence has also been reported in mammalian cells for an anti-apoptotic role for B'' and B subunit families (48). In this latter study Strack *et al.* (48) presented results of four different assays analyzing the importance of B55/B family subunits for cell survival. In seeming contrast to our results, one of the assays that showed little effect was small interfering RNA knockdown of B α . However, the efficiency of their B α knockdown was not reported, making comparison to our results difficult. Moreover, in concert with our data, results from two of their other three assays supported an anti-apoptotic role for B α . Our finding that B α down-regulation induces a small amount of apoptosis that is dependent on progression through mitosis is also consistent with the ability of the adenovirus protein, E4orf4, to arrest cells in G₂/M and induce apoptosis in cancer cells in a manner dependent on its ability to bind PP2A B α (51–54). Our results indicate a pro-survival function for LCMT-1 as well. This function may be mediated to some extent through modulation of PP2A_{B α AC} heterotrimer formation, but our data suggest that B α -independent roles should also be considered.

The fact that knockdown of either B α or LCMT-1 caused an enhancement of cell killing by nocodazole in HeLa cells raises the possibility that B α heterotrimers and LCMT-1 may have potential as targets for combination chemotherapy with microtubule targeting drugs like taxanes. Importantly, both B α and LCMT-1 knockdown HeLa cells were greatly protected from cell death by arrest in G₁/S, presumably by blocking the progression of the knockdown cells into mitosis, where apoptosis was triggered due to a defective spindle checkpoint. One would expect that knockdown of these proteins would not have the same sensitizing effect to nocodazole in all cell types given that some cancer cells already have defects in checkpoints and cell cycle control. HCT116 cells also showed sensitization to nocodazole (Fig. 7). However, initial experiments with H1299 lung cancer cells gave a different result. Although these cells exhibit significant death when LCMT-1 is knocked down by either L2 or L3, this cell line is already more sensitive to nocodazole than HeLa or HCT116 cells and, not unexpectedly, does not show increased nocodazole sensitivity upon LCMT-1 knockdown by the L2 and L3 shRNAs (data not shown). Further experimentation will be necessary to investigate the potential of these proteins as novel drug targets.

Consistent with the observed effects of LCMT-1 reduction on cell viability, homozygous gene trap knock-out of LCMT-1 results in embryonic lethality. The expected ratio of LCMT-1^{+/+}: LCMT-1^{+/-}: LCMT-1^{-/-} progeny mice from a cross of LCMT-1^{+/-} mice is 1:2:1. We obtained a ratio of 1:1.4:0 (Fig. 8D) with sufficient numbers of progeny to clearly indicate that homozygous loss of LCMT-1 is lethal during development. This result could not arise simply from inviable gametes because both male and female LCMT-1^{+/-} mice are fertile when bred to wild-type mice.³ Based on our results with cells, this lethality could result from defects in cell cycle or increased apoptosis, but it is also possible that additional signaling defects may also contribute. To our knowledge this is the first report that LCMT-1 is essential for development. In addition, the lower than expected numbers of LCMT-1^{+/-} mice also raise the possibility that hemizygous loss of LCMT-1 may cause some embryonic lethality as well. Future experiments will be aimed at elucidating the nature and timing of developmental defects that lead to the death of embryos lacking this important methyltransferase enzyme.

³J. A. Lee and D. C. Pallas, unpublished information.

Acknowledgments

We are grateful to Dr. William Hahn and The RNAi Consortium at the Broad Institute for lentiviral shRNA vectors and advice, to Dr. David M. Virshup for the HA-tagged B α construct, to Dr. Eva Schmeltz for HCT116 cells, to the German Gene Trap Consortium for the LCMT-1^{+/-} embryonic stem cells, to David Martin and colleagues in the Emory Transgenic facility for help with the LCMT-1 knock-out, to William Dalton for advice on caspase assays, and to Anita Corbett and Jennifer Jackson for critical reading of the manuscript.

References

1. Janssens V, Goris J. *Biochem J.* 2001; 353:417–439. [PubMed: 11171037]
2. Pallas DC, Shahrik LK, Martin BL, Jaspers S, Miller TB, Brautigan DL, Roberts TM. *Cell.* 1990; 60:167–176. [PubMed: 2153055]
3. Yang SI, Lickteig RL, Estes R, Rundell K, Walter G, Mumby MC. *Mol Cell Biol.* 1991; 11:1988–1995. [PubMed: 1706474]
4. Sontag E, Fedorov S, Kamibayashi C, Robbins D, Cobb M, Mumby M. *Cell.* 1993; 75:887–897. [PubMed: 8252625]
5. Cayla X, Ballmer-Hofer K, Merlevede W, Goris J. *Eur J Biochem.* 1993; 214:281–286. [PubMed: 8389702]
6. Campbell KS, Auger KR, Hemmings BA, Roberts TM, Pallas DC. *J Virol.* 1995; 69:3721–3728. [PubMed: 7538174]
7. Glenn GM, Eckhart W. *J Virol.* 1995; 69:3729–3736. [PubMed: 7538175]
8. Ogris E, Gibson DM, Pallas DC. *Oncogene.* 1997; 15:911–917. [PubMed: 9285686]
9. Chen W, Possemato R, Campbell KT, Plattner CA, Pallas DC, Hahn WC. *Cancer Cell.* 2004; 5:127–136. [PubMed: 14998489]
10. Xie H, Clarke S. *J Biol Chem.* 1993; 268:13364–13371. [PubMed: 8514774]
11. Lee J, Stock J. *J Biol Chem.* 1993; 268:19192–19195. [PubMed: 8396127]
12. Xie H, Clarke S. *J Biol Chem.* 1994; 269:1981–1984. [PubMed: 8294450]
13. Favre B, Zolnierowicz S, Turowski P, Hemmings BA. *J Biol Chem.* 1994; 269:16311–16317. [PubMed: 8206937]
14. Li M, Damuni Z. *Biochem Biophys Res Commun.* 1994; 202:1023–1030. [PubMed: 8048914]
15. Floer M, Stock J. *Biochem Biophys Res Commun.* 1994; 198:372–379. [PubMed: 8292043]
16. De Baere I, Derua R, Janssens V, Van Hoof C, Waelkens E, Merlevede W, Goris J. *Biochemistry.* 1999; 38:16539–16547. [PubMed: 10600115]
17. Ogris E, Du X, Nelson KC, Mak EK, Yu XX, Lane WS, Pallas DC. *J Biol Chem.* 1999; 274:14382–14391. [PubMed: 10318862]
18. Xie H, Clarke S. *Biochem Biophys Res Commun.* 1994; 203:1710–1715. [PubMed: 7945320]
19. Lee J, Chen Y, Tolstykh T, Stock J. *Proc Natl Acad Sci U S A.* 1996; 93:6043–6047. [PubMed: 8650216]
20. Evans DR, Hemmings BA. *Mol Gen Genet.* 2000; 264:425–432. [PubMed: 11129046]
21. Bryant JC, Westphal RS, Wadzinski BE. *Biochem J.* 1999; 339:241–246. [PubMed: 10191253]
22. Tolstykh T, Lee J, Vafai S, Stock JB. *EMBO J.* 2000; 19:5682–5691. [PubMed: 11060019]
23. Wu J, Tolstykh T, Lee J, Boyd K, Stock JB, Broach JR. *EMBO J.* 2000; 19:5672–5681. [PubMed: 11060018]
24. Yu XX, Du X, Moreno CS, Green RE, Ogris E, Feng Q, Chou L, McQuoid MJ, Pallas DC. *Mol Biol Cell.* 2001; 12:185–199. [PubMed: 11160832]
25. Wei H, Ashby DG, Moreno CS, Ogris E, Yeong FM, Corbett AH, Pallas DC. *J Biol Chem.* 2001; 276:1570–1577. [PubMed: 11038366]
26. Gentry MS, Li Y, Wei H, Syed FF, Patel SH, Hallberg RL, Pallas DC. *Eukaryot Cell.* 2005; 4:1029–1040. [PubMed: 15947195]
27. Nunbhakdi-Craig V, Schuechner S, Sontag JM, Montgomery L, Pallas DC, Juno C, Mudrak I, Ogris E, Sontag E. *J Neurochem.* 2007; 101:959–971. [PubMed: 17394530]
28. Lee TH, Turck C, Kirschner MW. *Mol Biol Cell.* 1994; 5:323–338. [PubMed: 8049524]

29. Minshull J, Straight A, Rudner AD, Dernburg AF, Belmont A, Murray AW. *Curr Biol*. 1996; 6:1609–1620. [PubMed: 8994825]
30. Yellman CM, Burke DJ. *Mol Biol Cell*. 2006; 17:658–666. [PubMed: 16314395]
31. Wang Y, Ng TY. *Mol Biol Cell*. 2006; 17:80–89. [PubMed: 16079183]
32. Turowski P, Fernandez A, Favre B, Lamb NJ, Hemmings BA. *J Cell Biol*. 1995; 129:397–410. [PubMed: 7721943]
33. Zhu T, Matsuzawa S, Mizuno Y, Kamibayashi C, Mumby MC, Andjelkovic N, Hemmings BA, Onoe K, Kikuchi K. *Arch Biochem Biophys*. 1997; 339:210–217. [PubMed: 9056251]
34. Wang Y, Burke DJ. *Mol Cell Biol*. 1997; 17:620–626. [PubMed: 9001215]
35. Gil-Bernabe AM, Romero F, Limon-Mortes MC, Tortolero M. *Mol Cell Biol*. 2006; 26:4017–4027. [PubMed: 16705156]
36. Moffat J, Grueneberg DA, Yang X, Kim SY, Kloepfer AM, Hinkle G, Piqani B, Eisenhaure TM, Luo B, Grenier JK, Carpenter AE, Foo SY, Stewart SA, Stockwell BR, Hacohen N, Hahn WC, Lander ES, Sabatini DM, Root DE. *Cell*. 2006; 124:1283–1298. [PubMed: 16564017]
37. Kalhor HR, Luk K, Ramos A, Zobel-Thropp P, Clarke S. *Arch Biochem Biophys*. 2001; 395:239–245. [PubMed: 11697862]
38. Coleman ML, Sahai EA, Yeo M, Bosch M, Dewar A, Olson MF. *Nat Cell Biol*. 2001; 3:339–345. [PubMed: 11283606]
39. Kerr JF, Wyllie AH, Currie AR. *Br J Cancer*. 1972; 26:239–257. [PubMed: 4561027]
40. Tamaoki T, Nomoto H, Takahashi I, Kato Y, Morimoto M, Tomita F. *Biochem Biophys Res Commun*. 1986; 135:397–402. [PubMed: 3457562]
41. Garcia-Calvo M, Peterson EP, Leiting B, Ruel R, Nicholson DW, Thornberry NA. *J Biol Chem*. 1998; 273:32608–32613. [PubMed: 9829999]
42. Honkanen RE, Golden T. *Curr Med Chem*. 2002; 9:2055–2075. [PubMed: 12369870]
43. Kitajima TS, Sakuno T, Ishiguro K, Iemura S, Natsume T, Kawashima SA, Watanabe Y. *Nature*. 2006; 441:46–52. [PubMed: 16541025]
44. Yan Y, Shay JW, Wright WE, Mumby MC. *J Biol Chem*. 1997; 272:15220–15226. [PubMed: 9182545]
45. Silverstein AM, Barrow CA, Davis AJ, Mumby MC. *Proc Natl Acad Sci U S A*. 2002; 99:4221–4226. [PubMed: 11904383]
46. Li X, Scuderi A, Letsou A, Virshup DM. *Mol Cell Biol*. 2002; 22:3674–3684. [PubMed: 11997504]
47. Chatfield K, Eastman A. *Biochem Biophys Res Commun*. 2004; 323:1313–1320. [PubMed: 15451440]
48. Strack S, Cribbs JT, Gomez L. *J Biol Chem*. 2004; 279:47732–47739. [PubMed: 15364932]
49. Ray RM, Bhattacharya S, Johnson LR. *J Biol Chem*. 2005; 280:31091–31100. [PubMed: 15994315]
50. Bonness K, Aragon IV, Rutland B, Ofori-Acquah S, Dean NM, Honkanen RE. *Mol Cancer Ther*. 2006; 5:2727–2736. [PubMed: 17121919]
51. Shtrichman R, Sharf R, Barr H, Dobner T, Kleinberger T. *Proc Natl Acad Sci U S A*. 1999; 96:10080–10085. [PubMed: 10468565]
52. Shtrichman R, Kleinberger T. *J Virol*. 1998; 72:2975–2982. [PubMed: 9525619]
53. Marcellus RC, Chan H, Paquette D, Thirlwell S, Boivin D, Branton PE. *J Virol*. 2000; 74:7869–7877. [PubMed: 10933694]
54. Shtrichman R, Sharf R, Kleinberger T. *Oncogene*. 2000; 19:3757–3765. [PubMed: 10949930]

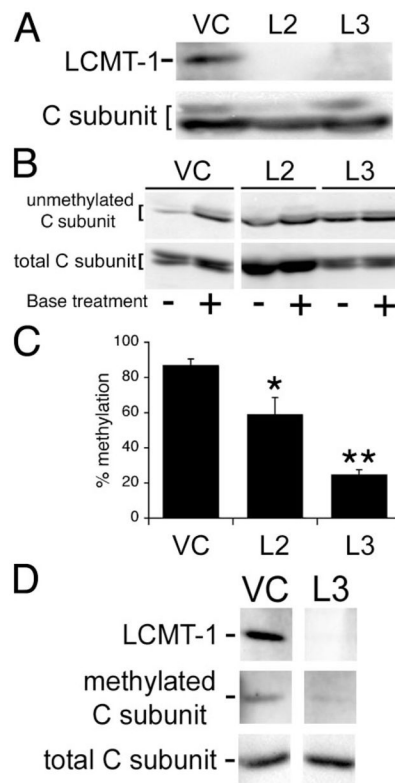


FIGURE 1. Analysis of LCMT-1 knockdown and PP2A methylation in LCMT-1 shRNA HeLa cells

A, two different LCMT-1 shRNAs (*L2* and *L3*) efficiently knockdown LCMT-1 protein levels in HeLa cells. VC cells and cells stably expressing the *L2* and *L3* LCMT-1 shRNAs were lysed, and lysates were probed for the steady-state levels of LCMT-1 and PP2A C subunit (C subunit; loading control) by immunoblotting. *B*, knockdown of LCMT-1 by expression of *L2* or *L3* shRNAs reduces PP2A C subunit methylation in HeLa cells. VC cells and LCMT-1 *L2* and *L3* shRNA cells were lysed, and the steady-state level of PP2A methylation in each cell line was determined using our previously published assay (24). Briefly, because base treatment demethylates the PP2A catalytic subunit, one aliquot of lysate from each line was treated for 5 min at 4 °C with 0.2 N NaOH to completely demethylate PP2A C subunit and was then neutralized (+lanes; 100% demethylated control), whereas another equal aliquot of lysate from each line was combined with preneutralized buffer (–lanes reflect endogenous methylation level). Then the untreated and base-treated aliquots were analyzed side by side on a 10% SDS-polyacrylamide gel followed by immunoblotting with a monoclonal antibody (4b7) specific for unmethylated C subunit. Demethylation of PP2A C subunit induced by *L2* and *L3* shRNA expression can be seen as an increase in the relative intensity of 4b7 signal in the minus versus plus lanes as compared with vector control cells. Also shown is an immunoblot of total PP2A C subunit showing that each pair of – and +lanes was loaded equally. *C*, the percent unmethylated PP2A catalytic subunit was determined by quantitatively comparing the amount of 4b7 signal in untreated samples (reflects level of endogenous unmethylated PP2A C subunit in each line) to that in the matched base-treated samples (100% demethylated controls) using a Bio-Rad Fluor-S Max Chemilumimager. Percent methylation was calculated by subtracting the percent of unmethylated PP2A from 100. The graph shows the averages and S.D. (error bars) of three independent experiments. Asterisks indicate significance versus vector control as assayed by *t* test (*, $p = 0.0499$; **, $p = 0.0001$). The C subunit can migrate as either

singlets or doublets; whether double or single bands are seen can vary for the same sample from gel to gel. This pattern of migration in SDS-PAGE has been noted previously for endogenous PP2A C subunits (6, 8, 24, 32) and does not appear to be due to degradation. *D*, immunoblotting with the anti-methylated PP2A catalytic subunit antibody, 2A10, further strengthens the conclusion that LCMT-1 is the major PP2A methyltransferase *in vivo*. Lysates prepared from VC and L3 LCMT-1 knockdown cells were analyzed by immunoblotting with LCMT-1 antibody to demonstrate LCMT-1 knockdown and with 2A10 monoclonal antibody (*methylated C subunit*) to show L3 LCMT-1 knockdown causes a substantial reduction in PP2A catalytic subunit methylation. Also shown is an immunoblot of total PP2A C subunit showing that the lanes were loaded equally. Quantitation of the 2A10 signals from two separate experiments showed that there was greater than a 3-fold reduction in methylation in the L3 LCMT-1 shRNA knockdown cells.

\$watermark-text

\$watermark-text

\$watermark-text

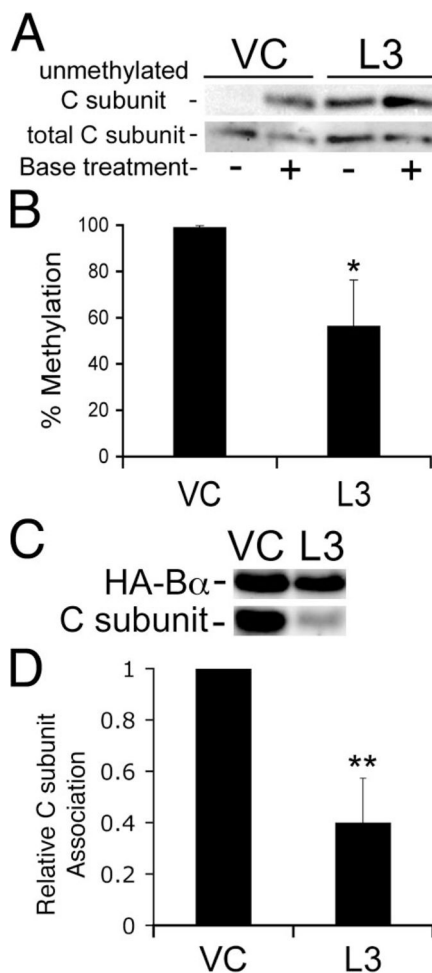


FIGURE 2. LCMT-1 knockdown reduces C subunit-B α association

VC cells and cells stably expressing an shRNA directed against LCMT-1 (L3) were transfected with a construct expressing HA-tagged B α (HA-B α) or an empty vector. *A*, the steady-state level of PP2A methylation in VC and L3 lysates (5% of the input of each immunoprecipitate) was determined using our previously described assay using our 4b7 methylation-sensitive monoclonal antibody (see the legend for Fig. 1*B*). The reduction in methylation induced by expression of the L3 shRNA can be seen by the increased signal in the *-lane*. Also shown is an immunoblot of total PP2A C subunit showing that each pair of *-* and *+* lanes was loaded equally. *B*, percent methylation of the PP2A catalytic subunit was determined as described in the legend to Fig. 1*C*. The graph shows the averages and S.D. (*error bars*) of three independent experiments. The *asterisk* indicates significance *versus* vector control as assayed by *t* test (*, $p = 0.02$). *C*, HA-B α immunoprecipitates of VC and L3 shRNA cells were probed for HA-tagged B α (HA-B α) and C subunit. The image shown is a representative immunoblot of three independent experiments. *D*, each band in *panel C* was quantitated using a Bio-Rad Fluor-S Max Chemilumimager. The relative amount of C subunit bound to HA-B α (*Relative C subunit association*) was calculated as a measure of the efficiency of C subunit association with HA-B α . The graph shown displays the average C subunit association with HA-B α in the three experiments. *Error bars* show S.D. of the three independent experiments. *Asterisks* indicate significance *versus* vector control as assayed by *t* test (**, $p = 0.0038$).

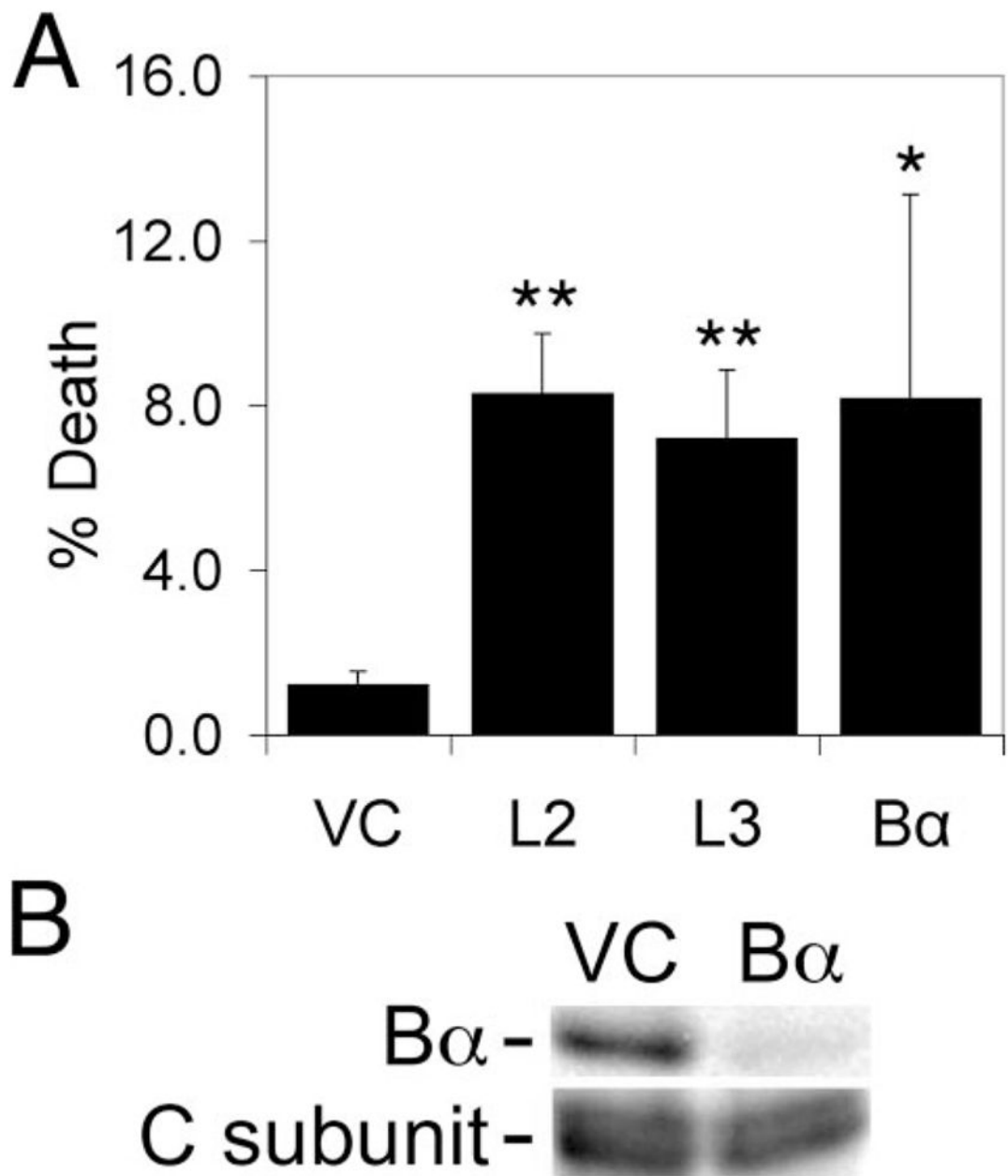


FIGURE 3. LCMT-1 or B α knockdown causes cell death

A, asynchronous VC cells, LCMT-1 shRNA knockdown cells expressing one of two different shRNAs to LCMT-1 (*L2* or *L3*), and PP2A B α regulatory subunit knockdown cells (*B α*) were plated and allowed to adhere, washed to remove dead cells, and then harvested after 24 h and assayed for viability by trypan blue exclusion. *Error bars* show S.D. of five independent experiments. *Asterisks* indicate significance *versus* vector control as assayed by *t* test (*L2****, p* = 0.000005; *L3****, p* = 0.00004; *B α* **, p* = 0.014). **B**, PP2A B α shRNA dramatically reduces B α protein levels in HeLa cells. VC cells, cells stably expressing shRNAs directed against B α were lysed, and lysates were probed for the steady-state levels of B α and PP2A C subunit (loading control) by immunoblotting.

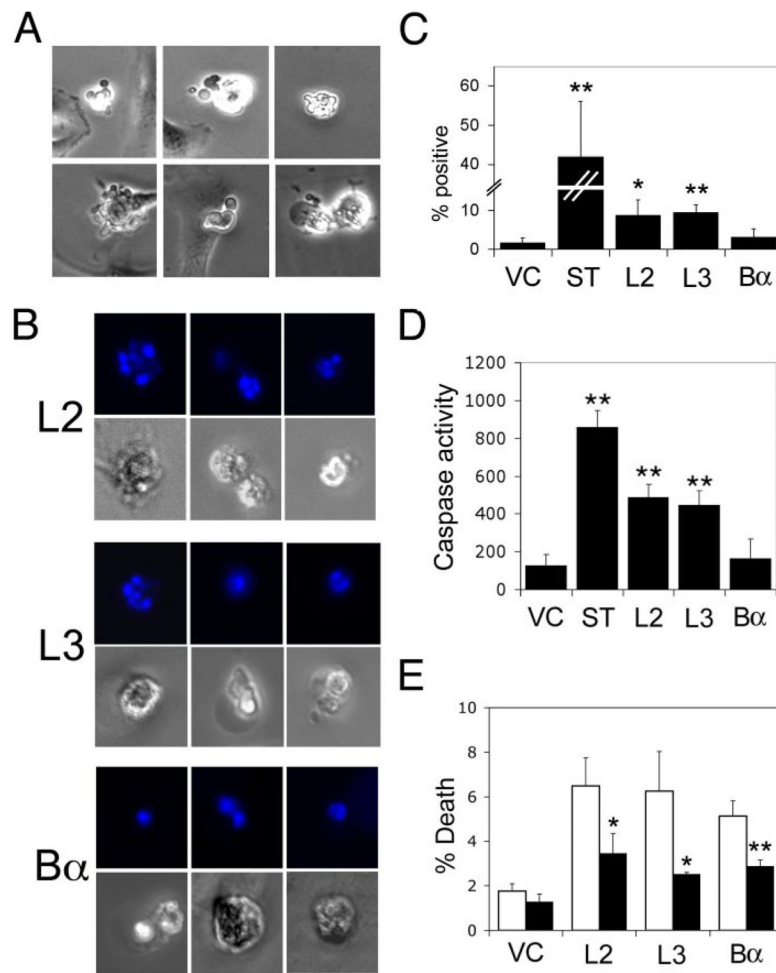


FIGURE 4. Characterization of cell death induced by knockdown of LCMT-1 or B α
A, LCMT-1 knockdown causes membrane blebbing. Asynchronous LCMT-1 shRNA knockdown cells (L2) were observed for 24–36 h by phase time-lapse microscopy. Six representative images of membrane blebbing in L2 knockdown cells are shown. **B**, knockdown of LCMT-1 or B α causes DNA condensation and fragmentation in HeLa cells. Asynchronous unselected VC cells (data not shown), LCMT-1 shRNA knockdown cells (L2 or L3), and B α knockdown cells infected with a multiplicity of infection of 3 were incubated with DAPI DNA stain to detect DNA condensation and fragmentation by immunofluorescence microscopy. Three representative images (*top row*, DAPI image; *bottom row*, differential interference contrast image) are shown for each cell line. **C**, LCMT-1 knockdown HeLa cells contain active caspases. Twenty-four hours after removal of dead cells by washing, asynchronous untreated VC cells, staurosporine-treated vector control cells (ST; positive control), LCMT-1 shRNA knockdown (L2 or L3), and B α knockdown cells were harvested, incubated with Red-DEVD-fmk (Calbiochem) for 1 h at 37 °C, and assayed by immunofluorescence microscopy. Error bars show S.D. of results obtained from a minimum of three fields. Asterisks indicate significance versus vector control as assayed by *t* test (*, $p=0.021$; **, $p=0.002$). Similar results were obtained in two independent experiments. **D**, LCMT-1 knockdown HeLa cell lysates exhibit caspase activity. The same cells as used in *panel C* were harvested, lysed by sonication, and incubated with z-DEVD-AFC (Calbiochem) for 1 h at 37 °C and assayed for caspase activation using a fluorimeter. Caspase activity shown is in relative fluorescence units. *Error*

bars show S.D. of results obtained triplicate wells. *Asterisks* indicate significance *versus* vector control as assayed by *t* test (ST^{**} , $p=0.0003$; $L2^{**}$, $p=0.003$; $L3^{**}$, $p=0.004$). Similar results were obtained in three independent experiments, except that $B\alpha$ had a statistically significant increase in caspase activity in one experiment. *E*, caspase inhibitor partially rescues cell death in LCMT-1 and $B\alpha$ knockdown cells. The same cells as used in *panel C* were plated into duplicate plates, and dead cells were removed by washing. One plate of cells was treated with $50\ \mu\text{M}$ z-VAD-fmk for 24 h, whereas the other was treated with vehicle only. Then the cells were harvested and assayed for trypan blue exclusion. A decrease in cell death in z-VAD-fmk-treated cells (*black bars*) as compared with untreated cells (vehicle control; *white bars*) can be seen. *Error bars* show S.D. of triplicate wells. *Asterisks* indicate significance *versus* vector control as assayed by *t* test ($L2^*$, $p=0.027$; $L3^*$, $p=0.022$; $**$, $p=0.006$). Similar results were obtained in two independent experiments.

\$watermark-text

\$watermark-text

\$watermark-text

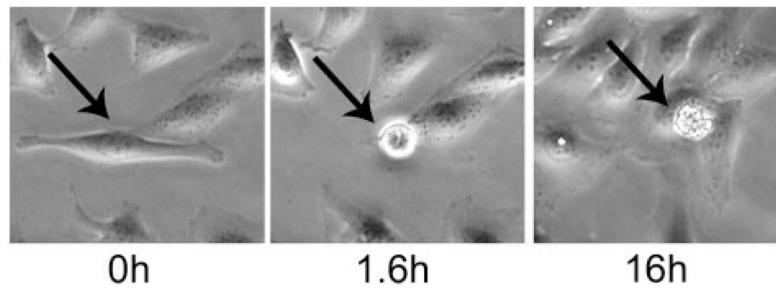


FIGURE 5. Some LCMT-1 knockdown cells die after entering mitosis

Asynchronous VC cells, LCMT-1 shRNA knockdown cells (L2 or L3), and B α subunit knockdown cells were observed for 24–36 h by phase time-lapse microscopy. A representative image of L3 knockdown cells at 0, 1.6, and 16 h is shown. The *black arrow* indicates the cell of interest through three panels. The metaphase plate (*vertical white line*) of this cell is visible in the *middle panel* (1.6-h time point).

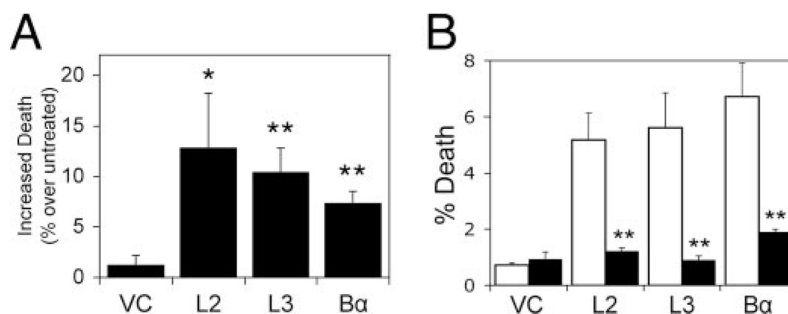


FIGURE 6. LCMT-1 or Ba reduction causes nocodazole sensitivity in HeLa cells

A, VC control HeLa cells, LCMT-1 shRNA knockdown cells (*L2* or *L3*), and *Ba* shRNA cells were plated into duplicate plates, and dead cells were removed by washing. One plate of cells was treated with nocodazole for 24 h, whereas the other was treated with vehicle only. Then the cells were harvested and assayed for trypan blue exclusion. Shown is the net increase in cell death for each line resulting from nocodazole treatment (% death of each line in nocodazole minus the % death of the same line in vehicle control). Error bars show S.D. of three different experiments. Asterisks indicate significance versus vector control as assayed by *t* test (*, $p = 0.022$; *L3*** $p = 0.004$; *Ba*** $p = 0.002$). *B*, thymidine rescues cell death in LCMT-1 and *Ba* knockdown HeLa cells. The same cells as used in *panel A* were plated into duplicate plates, and dead cells were removed by washing. One plate of cells was treated with thymidine for 24 h, whereas the other was treated with vehicle only. Then the cells were harvested and assayed for trypan blue exclusion. Shown is the cell death in untreated (control; white bars) and thymidine-treated cells (black bars). Error bars show S.D. for triplicate wells. Asterisks indicate significance versus vector control as assayed by *t* test (*L2*** $p = 0.002$; *L3*** $p = 0.003$; *Ba*** $p = 0.002$). Similar results were obtained two independent experiments.

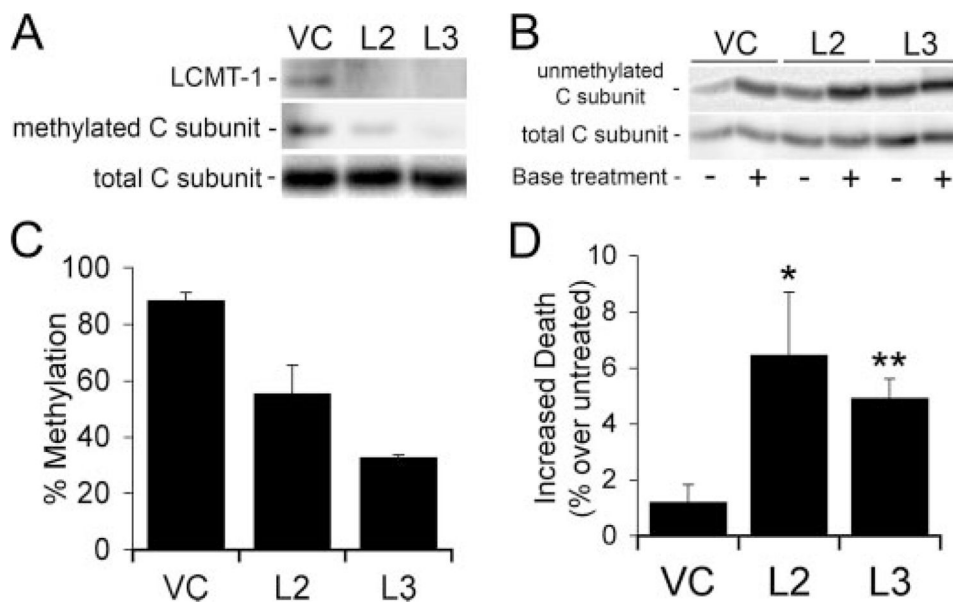


FIGURE 7. LCMT-1 knockdown in HCT116 colon cancer cells also causes decreased PP2A C subunit methylation and increased nocodazole sensitivity

A, two different LCMT-1 shRNAs (*L2* and *L3*) efficiently knockdown LCMT-1 protein levels and reduce PP2A C subunit methylation in HCT116 cells. Lysates from VC cells and cells stably expressing the *L2* and *L3* LCMT-1 shRNAs were probed by immunoblotting for the steady-state levels of LCMT-1 and PP2A C subunit methylation (methylated PP2A C subunit; using an anti-methyl PP2A C subunit monoclonal antibody, 2A10). Total PP2A C subunit was also immunoblotted as a loading control. *B*, the steady-state level of PP2A methylation in VC, *L2*, and *L3* lysates was also analyzed with our previously described assay using our 4b7 methylation-sensitive monoclonal antibody (see the legend for Fig. 1*B*). The untreated (–) and base-treated (+; 100% unmethylated control) aliquots were analyzed side by side on a 10% SDS-polyacrylamide gel followed by immunoblotting with 4b7, which is specific for unmethylated C subunit. Demethylation of PP2A C subunit induced by *L2* and *L3* shRNA expression can be seen as an increase in the relative intensity of 4b7 signal in the *minus versus plus lanes* of *L2* and *L3* as compared with the relative intensity of the *minus* and *plus lanes* in vector control. Also shown is an immunoblot of total PP2A C subunit showing that each pair of *minus* and *plus lanes* was loaded equally. *C*, quantitation of PP2A C subunit methylation reduction in HCT116 *L2* and *L3* LCMT-1 shRNA cells. The percent of unmethylated PP2A catalytic subunit in HCT116 cell lysates was determined by quantitatively comparing the amount of 4b7 signal in untreated samples (endogenous unmethylated PP2A C subunit) to that in the matched base-treated samples (100% demethylated controls) using a Bio-Rad Fluor-S Max Chemilumimager. Percent methylation was calculated by subtracting the percent of unmethylated PP2A from 100. The graph shows the averages of the results from two assays \pm range. *D*, LCMT-1 knockdown in HCT116 cells causes increased sensitivity to nocodazole. HCT116 VC and *L2* and *L3* LCMT-1 shRNA knockdown cells were plated into duplicate plates, and dead cells were removed by washing. One plate of cells was treated with nocodazole for 24 h, whereas the other was treated with vehicle only. Then the cells were harvested and assayed for trypan blue exclusion. Shown is the net increase in cell death for each line resulting from nocodazole treatment (% death of each line in nocodazole minus % death of the same line in vehicle control). Percent death in the absence of nocodazole in this experiment was: VC, 1.74 ± 0.43 ; *L2*, 9.2 ± 1.5 , $p = 0.012$; *L3*, 3.9 ± 0.7 , $p = 0.025$. Error bars show S.D. for triplicate wells. Asterisks indicate significance versus vector control as assayed by *t* test (*, $p = 0.028$;

** $, p = 0.002$). Similar results were obtained in three independent experiments, except in one case the p value for L3 was 0.06.

\$watermark-text

\$watermark-text

\$watermark-text

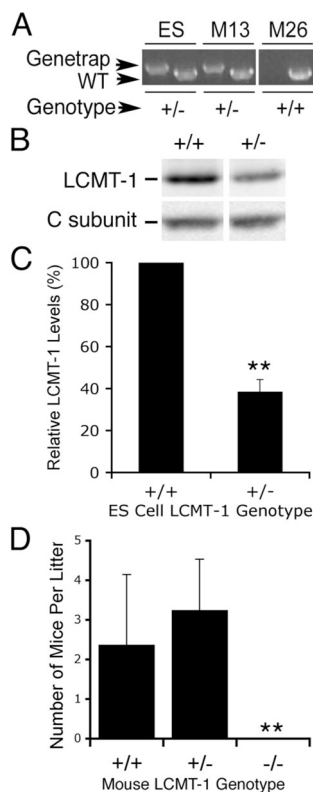


FIGURE 8. Homozygous knock-out of LCMT-1 in mice is embryonic lethal

A, DNA was prepared from LCMT-1^{+/-} mouse ES cells obtained from The German Gene Trap Consortium and from progeny mice (*M13*, *M26*) obtained from crossing of chimeric knock-out mice with C57BL/6 breeders. Each DNA was used in two PCR reactions, one using a primer pair specific for the wild-type LCMT-1 gene (*WT*; if positive, it indicates at least one LCMT-1 allele without gene trap insertion is present) and another using a primer pair specific for LCMT-1 having the gene trap insertion (Genetrap; forward primer matching the LCMT-1 intron and reverse primer matching the gene trap insert). Strong bands specific for the LCMT-1 Genetrap knock-out are seen in the LCMT-1^{+/-} ES cells (control) and in the LCMT-1^{+/-} mouse (*M13*), whereas the LCMT-1^{+/+} mouse (*M26*) clearly lacks the knock-out allele. **B**, LCMT-1 protein level is reduced in the LCMT-1^{+/-} ES cells. Equal numbers of LCMT-1^{+/-} ES cells (+/-) and control parental ES cells (+/+) were lysed and analyzed by SDS-PAGE and immunoblotting with LCMT-1 antibody. **C**, the results from one experiment from Fig. 7B performed in triplicate were quantitated, and the average and S.D. of the LCMT-1 levels in the LCMT-1^{+/-} ES cells normalized to the control LCMT-1^{+/+} ES cells are shown. Two separate experiments showed a reduction of >50%. **D**, no pups with homozygous gene trap knock-out of LCMT-1 were obtained from LCMT-1^{+/-} × LCMT-1^{+/-} mouse crosses. Eight crosses of LCMT-1^{+/-} × LCMT-1^{+/-} mice were performed, and pups were genotyped. Forty-five pups were obtained, 19 of which were LCMT-1^{+/-} and 26 of which were LCMT-1^{-/-}. No LCMT-1^{-/-} mice were obtained. Shown are the average number of pups in each litter that were LCMT-1^{+/+}, LCMT-1^{+/-}, or LCMT-1^{-/-}. Error bars indicate S.D. Asterisks indicate 99.8% confidence determined by *t* test that homozygous knock-out of LCMT-1 causes embryonic lethality (*p* = 0.002).